

# Contribution of chemoautotrophy and heterotrophy to the microbial carbon cycle in the Southwestern Atlantic Ocean

Julia Gasparini Passos<sup>1,\*</sup>, Luiza Ferreira Soares<sup>1</sup>, Paulo Yukio Gomes Sumida<sup>1</sup>, Amanda Gonçalves Bendia<sup>1</sup>, Fernanda Mancini Nakamura<sup>1</sup>, Vivian Helena Pellizari<sup>1</sup>, Camila Negrão Signori<sup>1</sup>

<sup>1</sup> Universidade de São Paulo, Instituto Oceanográfico (Praça do Oceanográfico, 191, 05508-120, São Paulo-SP, Brazil)

\* Corresponding author: [jpassos@usp.br](mailto:jpassos@usp.br)

## ABSTRACT

Dark carbon fixation (DCF) is a source of new and labile carbon in the deep ocean, while heterotrophic microbial production (HMP) promotes organic matter transfer through the microbial loop. Despite their ecological relevance, there is a scientific gap regarding the estimates of DCF and HMP in the Southwestern Atlantic Ocean. Thus, the aim of this study was to investigate the spatial distribution of DCF and HMP; their relevance to the ocean carbon cycle; their relationship with environmental parameters and amongst themselves on the upper slope of Santos Basin. The samples were collected at three different water depths and sediment layers aboard the R/V Alpha Crucis in November 2019. DCF and HMP rates were measured by <sup>14</sup>C-bicarbonate and <sup>3</sup>H-leucine incorporation, respectively, and incubated in the dark. In the water column, DCF rates varied from  $1.51 \times 10^1$  to  $3.24 \times 10^2 \mu\text{g C m}^{-3} \text{ h}^{-1}$ , which were one to two orders of magnitude lower than the HMP rates, from  $1.26 \times 10^2$  to  $1.48 \times 10^4 \mu\text{g C m}^{-3} \text{ h}^{-1}$ . In the sediments, the DCF ranged from  $1.15 \times 10^4$  to  $1.83 \times 10^5 \mu\text{g C m}^{-3} \text{ h}^{-1}$ , while HMP was one to four orders of magnitude lower,  $3.22 \times 10^1$  to  $1.56 \times 10^3 \mu\text{g C m}^{-3} \text{ h}^{-1}$ . DCF rates were significantly higher in the sediments, due to a higher availability of energy sources than in the oligotrophic water above. The HMP had higher rates in the water column as it is deeply dependent on organic matter derived from photosynthesis. This is the first study to investigate DCF and HMP considering the water column and sediments of the Southwestern Atlantic Ocean, thus contributing to a better understanding of the microbial role in the marine carbon cycle and ecosystem functioning.

**Descriptors:** Dark carbon fixation, Microbial loop, Marine carbon cycle, Pelagic and benthic microbial processes.

## INTRODUCTION

The deep sea, defined as the ocean lying below 200 m depth, is a highly connected environment; however, it remains undersampled, particularly in the southern hemisphere (Levin et al., 2019; Frazão et al., 2021). A recent review on

microbial ecology in the ocean reported that there are only 38 studies in the ocean basins of the southern hemisphere, compared with 290 studies conducted in the North Atlantic Ocean (Frazão et al., 2021).

The deep ocean plays a critical role in global biogeochemical cycles and hosts key marine ecosystem functions and services (Levin et al., 2019). While carbon fixation through photosynthesis has been always in the spotlight, the light-independent process of carbon fixation has been increasingly

Submitted: 30-Mar-2022

Approved: 30-Dec-2022

Associate Editor: Orlemir Carrerette



© 2022 The authors. This is an open access article distributed under the terms of the Creative Commons license.

studied and has proved to be relevant for the carbon cycle in the water column (Reinthal et al., 2010; Bergauer et al., 2013; Zhou et al., 2017; La Cono et al., 2018), in deep-sea sediments (Das et al., 2011; Molari et al., 2013), hydrothermal vents and cold seeps (Pimenov et al., 2000; McNichol et al., 2018; Savvichev et al., 2018).

Not only phytoplankton are able to carry out primary production, but also bacteria and archaea through chemosynthesis (Baltar and Herndl, 2019). Chemoautotrophic prokaryotes fix inorganic carbon by oxidizing reduced inorganic compounds, e.g.  $\text{NO}_2^-$ ,  $\text{NH}_4^+$  and  $\text{S}^2$  (Middelburg, 2011; Dyskma et al., 2016; Pachiadaki et al., 2017), with five distinctive  $\text{CO}_2$  assimilation pathways, e.g. Calvin-Benson-Bassham (CBB) cycle, reductive tricarboxylic acid (rTCA) cycle, Wood-Ljungdahl (WL) pathway, 3-hydroxypropionate bi-cycle (3-HP) and 3-hydroxypropionate/4-hydroxybutyrate cycle (3-HP/4-HB) (Hügler and Sievert, 2011). The chemoautotrophic process results in the production of new and labile organic carbon in environments otherwise dominated by refractory organic carbon (Middelburg, 2011), influencing the overall nitrogen, sulfur and carbon cycles in the oceans, and should be seen as an integral part of global primary production, since its addition would increase total oceanic primary production by 5-22% (Baltar and Herndl, 2019).

In the water column of the dark ocean, chemoautotrophy depends on the oxidation of nitrogen compounds mainly by nitrite-oxidizing bacteria and ammonia-oxidizing archaea (Middelburg, 2011; Pachiadaki et al., 2017), with a small contribution of oxidation of reduced sulfur compounds (Middelburg, 2011; Bendia et al., 2021). According to Hügler and Sievert (2011), the most common carbon fixation pathways in the euphotic zone are through CBB and 3HP/4HB, and in the mesophotic zone are CBB, 3HP/4HB and rTCA. In sediment, chemoautotrophy is mostly due to the oxidation of sulfur compounds, in particular sulfide by sulfur-oxidizing Gammaproteobacteria (Middelburg, 2011; Dyskma et al., 2016), with a lower impact of the oxidation of nitrogen compounds (Dyskma et al., 2016), mostly represented by archaea of the Nitrososphaeria class in the surface sediments of the Southwestern (SW) Atlantic Ocean (Bendia et

al., 2021; Bendia et al., 2022, this issue). The few studies on the preferential metabolic pathway of chemoautotrophs in sediments focus on regions of deeply buried marine sediments and point to rTCA and WL as a primordial carbon fixation pathway (Hügler and Sievert, 2011).

Heterotrophic bacteria and archaea, known to depend on the energy of organic matter in the microbial loop, consume the dissolved organic carbon derived from the primary production, which otherwise would be lost, and reincorporate it into the food chain (Azam et al., 1983), thus promoting organic matter transfer and energy flow from the bottom of the microbial loop. However, the heterotrophs can also fix  $\text{CO}_2$  through pathways involved in anaplerotic reactions of the tricarboxylic acid (TCA) cycle, synthesizing fatty acids, nucleotides and amino acids (Alonso-Sáez et al., 2010). The extent of anaplerotic reactions is largely determined by the availability of labile organic carbon (Reinthal et al., 2010), as key anaplerotic enzymes increase proportionally by sudden input of organic matter (Baltar et al., 2016). Measurements of  $\text{CO}_2$  fixation by heterotrophic bacterioplankton are scarce; however, previous studies suggest that about 1–8 % of the biomass production in heterotrophic bacteria is derived from anaplerotic reactions (Romanenko, 1964; Sorokin, 1993).

In the marine environment, the recent focus of chemoautotrophic studies has been in the water column and mainly concentrated in the northern hemisphere. Only a few studies combining chemosynthetic production (herein referred to as dark carbon fixation, DCF) and heterotrophic microbial production (HMP) have been done in the SW Atlantic Ocean. However, these published studies are only related to tropical estuarine systems (Signori et al., 2018; Signori et al., 2020). Thus, there is a need to increase the efforts in studies on these metabolic processes to better understand their impact on biogeochemical cycles as a whole. The aim of our study was to determine rates of DCF and HMP in the Santos Basin (SW Atlantic Ocean), and to test the hypothesis that DCF is a relevant process of the carbon cycle in the water column and sediments by comparing both processes throughout the pelagic and benthic zones, and between the ecological regions. Additionally,

we explored the spatial variability of DCF and HMP in relation to several environmental parameters.

## METHODS

### STUDY AREA AND SAMPLING STRATEGY

Sampling was carried out by the R/V Alpha Crucis of the Oceanographic Institute of the University of São Paulo (IOUSP), during November 11–24<sup>th</sup>, 2019 (Table S1) as part of the Bioil Project - Biology and Geochemistry of Oil and Gas Seepages, Southwest Atlantic (Sumida et al., 2022), coordinated by IOUSP and funded by Shell Brasil Petróleo LTDA. The study area comprises isobaths from 400 to 800 m depth on the upper slope of Santos Basin (SW Atlantic Ocean) (Figure 1), which is strongly influenced by the poleward flowing Brazil Current (BC), carrying the Tropical Water (TW) and South Atlantic Central Water (SACW) (Silveira et al., 2000). Below the BC flow, the Intermediate Western Boundary Current (IWBC), with a flow towards the equator, carries the Antarctic Intermediate Water (AAIW) (Boebel et al., 1997).

The 12 selected stations were strategically divided into three areas with different geomorphological features: Area 1 (A1, stations ST 681, ST 682, ST 683 and ST 684) with greater potential for active pockmarks (Maly et al., 2019); Area 2 (A2, stations ST 685, ST 686, ST 687 and ST 688) associated with the Alpha Crucis Carbonate Mound (Maly et al., 2019); and Area 3 (A3, stations ST 690, ST 691, ST 692 and ST 693) associated with pockmarks and salt diapirs (Schattner et al., 2016; de Mahiques et al., 2017; Schattner et al., 2018; Ramos et al., 2019). In total, 186 water samples and 187 sediment samples were collected. However, due to logistical problems, HMP was not analyzed for station ST 688 in A2, nor for the stations included in A3 (ST 690, ST 691 and ST 692).

Water samples were collected at three different depths, corresponding to surface (~40 m), intermediate (~250 m) and deep water (~600 m), using a Sea-Bird CTD/Carrousel 911 system equipped with 12 10 L Niskin bottles for the determination of DCF and HMP and nutrient analyses.

Sediment samples were collected with a box corer (50 cm x 50 cm x 50 cm, Ocean Instruments®). The overlying water was drained before opening the box corer; the cores were subsampled at 0–5, 5–10, and 10–15 cm layers for onboard DCF and HMP incubations. In addition, separate cores were also subsampled for geochemical analysis (total organic carbon, total nitrogen, carbonate content and the  $\delta^{13}\text{C}$ ). Sediments from the surface of each box corer were sampled for granulometric analysis and stored at -20°C.

### ENVIRONMENTAL PARAMETERS

Seawater temperature and salinity were measured *in situ* using the Sea-Bird CTD/Carrousel 911 system. For inorganic nutrients (phosphate, silicate, nitrate, nitrite and ammonium), approximately 20 L of each water sample were filtered onboard using a peristaltic pump and 0.22  $\mu\text{m}$ -membrane Sterivex™ filters. The filtered water samples used for chemical analyses were stored in amber flasks (for ammonium) and in 100 mL bottles (for other nutrients), which were immediately frozen at -80°C (adapted from Bertini & Braga, 2022). The nutrient analyses were performed in the “Nutrientes, Micronutrientes e Traços no Mar” laboratory at the Oceanographic Institute of the University of São Paulo (IOUSP). According to Grasshoff et al. (2009), phosphate, silicate and ammonium were analyzed using a spectrophotometer (Thermo Scientific Spectrophotometer Evolution 200), while nitrate and nitrite were determined using an autoanalyzer (SEAL Analytical AutoAnalyzer II).

Sediment granulometry was determined by a Malvern Mastersizer 2000 Laser Analyzer at the “Geologia de Margens Continentais” laboratory at IOUSP as described in the ISO system (ISO13320, 2009). Total organic carbon (TOC), total nitrogen (TN), and  $\delta^{13}\text{C}$  (reported in ‰ PDB) were determined by an elemental analyzer (EA - Costec) coupled to an isotopic ratio mass spectrometer (IRMS - Delta Advantage – Thermo Scientific) after acidification of samples with 2M HCl. The calcium carbonate content (reported in % of dry weight) was determined by gravimetric analyses before and after this acidification. Analyses of TOC, TN,  $\delta^{13}\text{C}$  and calcium carbonate were performed in the “Química Orgânica Marinha” laboratory at IOUSP.

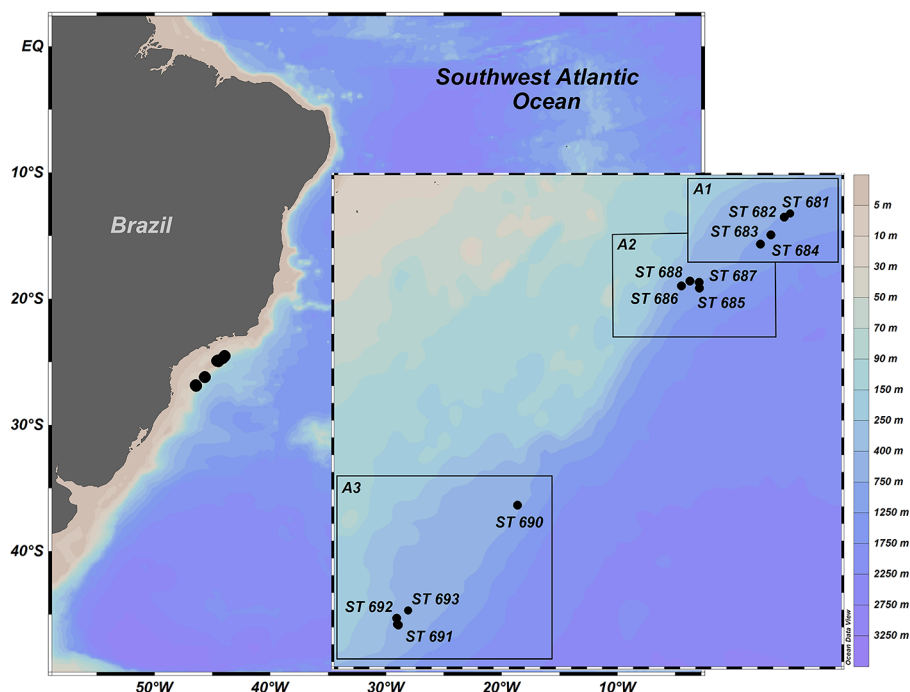


**Figure 1.** Map showing the location of sampling areas along the Santos Basin upper slope (SW Atlantic).

## DARK CARBON FIXATION

Rates of DCF in the water column and sediments were estimated using radiolabeled-inorganic carbon incorporation ( $^{14}\text{C}$ -bicarbonate), proposed by Steemann-Nielsen (1952) and Teixeira (1973), with slight modifications (Reinthal et al., 2010). Three samples, one blank and two sample replicates, of 50 ml (water) and 5 g (sediment) were incubated with 10  $\mu\text{Ci}$   $^{14}\text{C}$ -bicarbonate (specific activity 56  $\text{mCi mmol}^{-1}$ , Perkin Elmer, USA) in the dark at *in situ* temperature for 12 h. Before incubating, the sediment samples were combined with filtered water (0.22  $\mu\text{m}$ -membranes) and then homogenized to form a slurry; water samples were incubated without this step. At the end of the incubation, the water samples were filtered into 0.22  $\mu\text{m}$ -membranes using a vacuum pump and manifold, and the sediment samples were fixed with formaldehyde (2 % final concentration). To remove the remaining  $^{14}\text{C}$ -bicarbonate, the membranes and the fixed sediment were then exposed to concentrated HCl. Afterwards, at the “Laboratório Multiusuários de Radioisótopos do Departamento de Oceanografia Biológica” of IOUSP, each sample (membrane or sediment) was placed into

scintillation vials with 5 mL of scintillation cocktail (Optiphase Hisafe 3, Perkin Elmer). After being left in the dark for at least 24 h, the samples were counted for 30-60 minutes per sample, respectively, with the use of a liquid scintillation counter (Perkin Elmer Tricarb 2810 TR). The production rate of carbon per volume and time ( $\mu\text{g C m}^{-3} \text{ h}^{-1}$ ) was calculated as follows (Steemann-Nielsen, 1952; Teixeira, 1973):

$$DCF = \frac{\frac{DMP}{DMP_{add}} * 1.05 * \Sigma C_2 * \frac{12}{44}}{t}, \quad (1)$$

where, DPM and  $\text{DPM}_{add}$  are the disintegrations ( $\text{min}^{-1}$ ) of the sample and of the added  $^{14}\text{C}$ -bicarbonate, respectively; 1.05 is the isotopic effect  $^{14}\text{C}/^{12}\text{C}$ ;  $\Sigma\text{CO}_2 \times 12/44$  is the concentration of carbon from  $\text{CO}_2$  in the ocean,  $\Sigma\text{CO}_2$  considered to be 90,000  $\mu\text{g L}^{-1}$  (Steemann-Nielsen, 1952); and  $t$  is the total incubation time (h).

## HETEROTROPHIC MICROBIAL PRODUCTION

The HMP in the water column and sediments was estimated using the  $^3\text{H}$ -leucine incorporation method from Kirchman et al. (1985), and modified by Smith and Azam (1992), Svensson et al. (2001)

and Santoro et al. (2013). Five samples, two blanks and three sample replicates, of 1 ml (water) and 1 g (sediment) were placed into Eppendorfs with 10 nM  $^3\text{H}$ -leucine (specific activity 125.6 Ci mmol $^{-1}$ , Perkin Elmer, USA), and incubated in the dark at *in situ* temperature for 6 h. Before incubating, the sediment samples were combined with filtered water (0.22  $\mu\text{m}$ -membranes) and then homogenized to form a slurry; water samples were incubated without this step. All incubations were terminated by the addition of formaldehyde (2 % final concentration). At the “Laboratório Multiusuários de Radioisótopos do Departamento de Oceanografia Biológica”, the samples were treated with 5 % trichloroacetic acid, Milli-Q water and ethanol through successive steps of centrifugation for protein extraction. Subsequently, 1.5 ml of scintillation cocktail (Optiphase Hisafe 3, Perkin Elmer) was added to the Eppendorf, and after being left in the dark for at least 24 h, the water and sediment were counted for 30-60 minutes per sample, respectively, with the use of a liquid scintillation counter (Perkin Elmer Tricarb 2810 TR). The resulting disintegrations per minute (DPM) were converted into production rate of carbon per volume and time ( $\mu\text{g C m}^{-3} \text{ h}^{-1}$ ), using the equations 2 and 3. The moles of exogenous leucine incorporated was calculated as follows (Wetzel and Likens, 1991):

$$nmol_{inc} = \frac{DPM_{rep} - DPM_c}{\Delta E * 2.22 * 10^6}, \quad (2)$$

where  $DPM_{rep}$  and  $DPM_c$  are the disintegrations ( $\text{min}^{-1}$ ) of the replicate and the control, respectively;  $\Delta E$  is the radioisotope specific activity (Ci nmol $^{-1}$ ); and  $2.22 \times 10^6$  equals to the DPM in 1 Ci. To calculate the Bacterial Protein Production (BPP) from leucine incorporation, the following equation was used (Simon and Azam, 1989):

$$BBP = \frac{nmol_{inc}}{V * t} * \frac{100}{7.3} * 131.2 * ID, \quad (3)$$

where  $V$  is the volume (L) of the sample;  $t$  is the time of incubation (h);  $100/7.3$  is the 100/% of leucine in one protein molecule; 131.2 is the atomic weight of leucine; and  $ID$  is the intracellular isotope dilution of  $^3\text{H}$ -leucine, considered 2 by Smith and Azam (1992). Finally, BPP was converted into

HMP by considering the theoretical protein/carbon conversion factor of 0.86 (Simon and Azam, 1989).

## STATISTICAL ANALYSIS

The statistical differences in DCF and HMP rates between each area, water depth and sediment layer were tested using an analysis of variance (ANOVA) followed by Tukey’s post hoc multiple-comparison test. Normality of residuals was tested using the Shapiro-Wilk test, and a  $\log(x)$  transformation was applied when the data did not fit normality. The Levene’s test was used to test the homogeneity of variances using the “car 3.0-10” package (Fox and Weisberg, 2019). To analyze the relationship between DCF and HMP, a simple linear regression analysis on a log scale was performed. Additionally, a principal component analysis (PCA) was performed to the Pearson’s correlation matrix to reduce the dimensionality of the dataset and possibly ordination of the samples. Also, to validate the ordination observed in the PCA, a permutational multivariate analysis of variance (PERMANOVA) was carried out using the “vegan 2.5-7” package (Oksanen et al., 2020). All data analysis was conducted using R software (version 4.0.3; R core team, 2020).

## RESULTS

### ENVIRONMENTAL PARAMETERS

Seawater temperature and salinity decreased with depth, ranging from 4.6 to 24.7 °C and 34.3 to 37.2 psu, respectively (Table 1). According to the T-S diagram (Figure 2), we were able to observe the presence of the TW, SACW and AAIW, the latter only at the A1 (at the bottom of stations ST 683 and ST 684). In general, inorganic nutrient concentrations increased with depth, with phosphate, silicate and nitrate varying from 0.05 to 1.92  $\mu\text{mol L}^{-1}$ , 0.64 to 20.25  $\mu\text{mol L}^{-1}$  and 0.33 to 27.51  $\mu\text{mol L}^{-1}$ , respectively (Table 1). Concentrations of nitrite and ammonium showed a different trend, reaching their maximum at the intermediate depth, and ranging from 0.01 to 0.05  $\mu\text{mol L}^{-1}$  and 0.02 to 0.42  $\mu\text{mol L}^{-1}$ , respectively (Table 1).

**Table 1.** Environmental parameters of the water samples, including zones of water column, depth (m), temperature (°C), salinity (psu), and the nutrients phosphate, silicate, nitrate, nitrite and ammonium, all represented as  $\mu\text{mol L}^{-1}$ .

Station	Zone	Depth	Temperature	Salinity	Phosphate	Silicate	Nitrate	Nitrite	Ammonium
ST 682	Surface	45	24.5	37.2	0.05	0.69	0.36	0.02	0.14
	Intermediate	263	14.6	35.4	0.61	2.83	3.66	0.03	0.21
	Deep	701	5.4	34.3	1.83	15.91	21.67	0.02	0.11
ST 683	Surface	44	23.1	36.9	0.07	1.16	0.40	0.01	0.07
	Intermediate	283	12.9	35.1	0.58	5.55	06.04	0.03	0.16
	Deep	811	4.7	34.3	1.36	13.77	24.68	0.02	0.11
ST 684	Surface	40	23.5	36.9	0.09	5.61	1.48	0.02	0.05
	Intermediate	280	12.8	35.1	0.80	3.99	07.02	0.04	0.28
	Deep	804	4.6	34.3	1.92	20.25	27.51	0.02	0.14
ST 685	Surface	46	23.9	36.9	0.11	0.64	0.52	0.01	0.07
	Intermediate	282	13.3	35.2	0.88	3.47	9.00	0.04	0.38
	Deep	551	7.6	34.5	1.37	8.73	19.28	0.02	0.11
ST 686	Surface	40	24.6	37.2	0.05	0.98	0.33	0.02	0.11
	Intermediate	278	13.6	35.3	0.65	11.34	07.06	0.05	0.42
	Deep	530	8.4	34.6	1.58	6.74	21.37	0.02	0.16
ST 687	Surface	48	23.9	36.9	0.11	0.75	0.49	0.02	0.05
	Intermediate	280	12.5	35.1	0.89	3.93	9.21	0.03	0.30
	Deep	560	6.7	34.4	1.41	10.87	19.51	0.02	0.14
ST 688	Surface	45	23.8	36.8	0.20	1.10	0.74	0.02	0.11
	Intermediate	280	13	35.2	0.85	3.59	8.12	0.04	0.24
	Deep	530	8	34.5	01.09	6.88	13.15	0.02	0.09
ST 690	Surface	41	23.9	36.8	0.95	3.70	11.11	0.04	0.16
	Intermediate	280	12.6	35.1	0.17	0.87	0.59	0.02	0.11
	Deep	740	5.8	34.4	1.78	16.37	24.28	0.02	0.11
ST 691	Surface	49	24.5	37.2	0.18	0.64	0.62	0.02	0.14
	Intermediate	282	14.2	35.3	0.71	2.72	7.76	0.03	0.24
	Deep	513	10.5	34.8	1.26	6.77	17.47	0.02	0.16
ST 692	Surface	45	24.7	37.2	0.09	0.69	0.40	0.01	0.02
	Intermediate	280	13.7	35.3	0.72	3.70	6.96	0.02	0.14
	Deep	480	10.7	34.9	1.15	5.90	16.90	0.02	0.07
ST 693	Surface	45	23.5	36.6	0.09	1.10	0.42	0.02	0.05
	Intermediate	160	18.3	36	0.33	2.37	1.43	0.03	0.11
	Deep	380	11.5	35	01.08	5.32	11.87	0.03	0.25

Most stations sampled were characterized by sandy mud sediment, with A1 presenting the lower sand content among them. TOC and TN decreased with sediment depth, ranging from <LOD (limit of detection) to 1.74 % and <LOD to 0.17 %, respectively (Table 2). Carbonate content and the  $\delta^{13}\text{C}$  were similar throughout the sediment layers, from 3.38 to 13.78 % and -22.35 to -20.64 ‰.

(Table 2). Additionally, the A1 and A2 revealed a higher carbonate content.

## MICROBIAL PROCESSES

In the water column, the DCF rates varied from  $1.51 \times 10^1$  to  $3.24 \times 10^2 \mu\text{g C m}^{-3} \text{h}^{-1}$  (Table S2), showing no spatial pattern ( $p > 0.05$ ) in relation to depths (Figure 3A) or areas (Figure 3B). However,

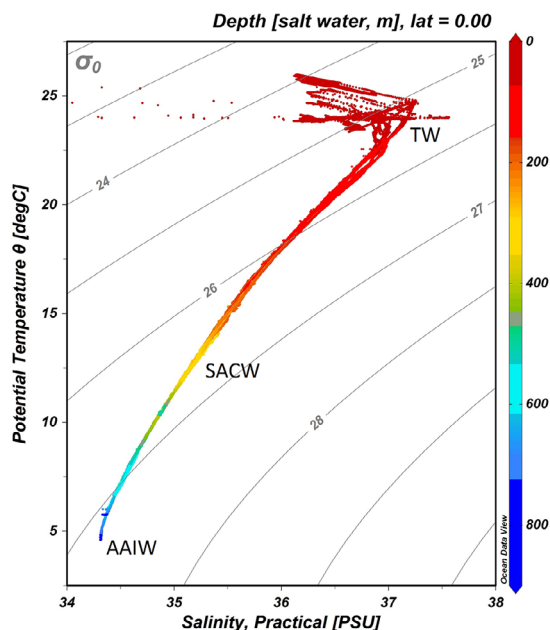


**Figure 2.** Temperature-salinity (TS) diagram in 800 m water depth in the Santos Basin during a spring cruise in November 2019. Water masses are labeled: Tropical Water (TW), South Atlantic Central Water (SACW) and Antarctic Intermediate Water (AAIW).

DCF rates were one to two orders of magnitude lower than the HMP rates, which ranged from  $1.26 \times 10^2$  to  $1.48 \times 10^4 \mu\text{g C m}^{-3} \text{h}^{-1}$  (Table S2), and also did not show a spatial pattern ( $p > 0.05$ ) (Figure 3C and 3D).

The DCF rates in the sediments ranged from  $1.15 \times 10^4$  to  $1.83 \times 10^5 \mu\text{g C m}^{-3} \text{h}^{-1}$  (Table S3), with no significant difference ( $p > 0.05$ ) between layers (Figure 4A). A2 presented significantly higher means of DCF than A3 ( $p < 0.05$ ) throughout all sediment layers, but A1 was not significantly different ( $p > 0.05$ ) from the other areas (Figure 4B). The DCF rates were one to four orders of magnitude higher than the HMP rates, which ranged from  $3.22 \times 10^1$  to  $1.56 \times 10^3 \mu\text{g C m}^{-3} \text{h}^{-1}$  (Table S3). No spatial pattern ( $p > 0.05$ ) was observed for HMP rates in sediments (Figure 4C and 4D).

When comparing microbial processes between water column and sediment, DCF rates were much higher in the sediment, with a difference of two orders of magnitude, while HMP rates were an order of magnitude higher in the water column than in the sediment.

## REGULATION OF THE MICROBIAL PROCESSES

The principal component analysis (PCA) was carried out in all our dataset to elucidate the variation of our samples, including environmental parameters and measured rates. The results for the water column revealed that two principal components explained 74.18 % of the sample variability. The first component (PC1) explained 55.64 % of the total variation and was more strongly correlated with depth ( $r = 0.41$ ), phosphate ( $r = 0.41$ ), temperature ( $r = -0.41$ ), nitrate ( $r = 0.40$ ), salinity ( $-0.40$ ) and silicate ( $r = 0.37$ ). The second component (PC2) explained 18.54 % of the total variation, being more strongly correlated with nitrite ( $r = 0.69$ ) and ammonium ( $r = 0.68$ ). Neither DCF nor HMP rates were shown to be significantly relevant to the overall sample variability shown in the PCA, as they were not strongly associated with the PCs. Figure 5 projects the data onto the span of the principal components and shows how the variables relate to the PCs. It shows an apparent separation between the surface, intermediate and deep water samples in the PC1-axis. The PC1 was associated with depth dependent variables, such as temperature and salinity (decreased with depth) and phosphate, silicate and nitrate (increased with depth). However, the variance of the intermediate water was mainly in the PC2-axis, which is associated with nutrients with peak concentration in this depth, like nitrite and ammonium. Yet, the ordination observed in Figure 5 was not confirmed by a permutational multivariate analysis of variance (PERMANOVA,  $R^2 = 0.005$ ,  $p = 0.97$ ). There was no apparent ordination observed regarding the areas (Figure 5), which was verified by the PERMANOVA ( $R^2 = 0.02$ ,  $p = 0.57$ ).

Regarding the sediments, the PCA revealed that two principal components explained 64.89 % of the sample variability. The first component (PC1) explained 36.92 % of the total variation and was more strongly correlated with TOC ( $r = 0.53$ ), TN ( $r = 0.5$ ), HMP ( $r = 0.48$ ) and  $\delta^{13}\text{C}$  ( $r = 0.30$ ). The second component (PC2) explained 27.96 % of the total variation, being more strongly correlated with sand ( $r = 0.62$ ), mud ( $r = -0.62$ ) and  $\text{CaCO}_3$  ( $r$

**Table 2.** Environmental parameters of the sediment samples, including layer (cm), sand and mud content, total organic carbon (TOC) (%), total nitrogen (TN) (%), carbonate content ( $\text{CaCO}_3$ ) (%) and the  $\delta^{13}\text{C}$  (‰). Lines containing a dash signify the absence of data in the corresponding layers.

Station	Layer	Sand	Mud	$\text{CaCO}_3$	TOC	$\delta^{13}\text{C}$	TN
ST 681	0-5	12.967	87.033	11.390	0.450	-20.860	0.070
	5-10	19.800	80.200	8.150	0.310	-21.360	0.050
	10-15	10.400	89.600	9.070	0.160	-22.150	0.020
ST 683	0-5	10.567	89.433	9.585	0.510	-21.070	0.035
	5-10	20.050	79.950	9.070	0.270	-21.650	0.010
	10-15	24.667	75.333	12.420	<0.01	-	<0.01
ST 684	0-5	14.625	85.375	8.883	0.4967	-21.063	0.070
	5-10	23.750	76.250	9.230	0.1500	-21.560	0.020
	10-15	22.700	77.300	9.640	<0.01	-	<0.01
ST 685	0-5	23.850	76.150	6.430	1.740	-20.820	0.170
	5-10	-	-	-	-	-	-
ST 686	0-5	29.233	70.767	6.485	0.475	-21.495	0.055
	5-10	44.450	55.550	7.820	0.240	-20.970	0.050
	10-15	32.100	67.900	5.120	0.320	-20.900	0.020
ST 687	0-5	13.750	86.250	4.990	0.540	-20.640	0.050
	5-10	25.050	74.950	13.780	0.300	-21.300	0.020
	10-15	28.433	71.567	8.270	0.190	-22.350	0.010
ST 688	0-5	34.700	65.300	7.275	0.565	-21.235	0.055
	5-10	47.450	52.550	5.220	0.450	-21.280	0.040
	10-15	45.200	54.800	-	-	-	-
ST 690	0-5	21.767	78.233	3.710	0.440	-22.130	<0.01
	5-10	29.850	70.150	3.530	0.420	-21.250	<0.01
	10-15	31.133	68.867	3.600	0.410	-21.830	<0.01
ST 691	0-5	26.633	73.367	4.635	0.380	-21.260	<0.01
	5-10	26.650	73.350	3.380	0.360	-22.280	<0.01
	10-15	-	-	-	-	-	<0.01

= -0.32). The DCF was not significantly relevant to the overall sample variability shown in the PCA, as it was not strongly associated with any PC. Figure 6 plots the data in function of the PCs and how the variables relate to them. Figure 6 shows that the variation occurring along the PC1-axis is associated with variables related with organic matter, such as TOC, TN, HMP and  $\delta^{13}\text{C}$ . Further, there is an apparent separation of A1 from the other areas along the PC2-axis, which is mainly dictated by grain-size and carbonate content. This ordination between areas in Figure 6 has shown to be significant (PERMANOVA,  $p = 0.03$ ), representing 25.17 % ( $R^2 = 0.25$ ) of the variation. In addition, no

ordination among layers was observed (Figure 6, PERMANOVA,  $R^2 = 0.005$ ,  $p = 0.94$ ).

A Pearson correlation coefficient was determined to assess the relationship between the measured rates and the environmental parameters. For the water column, neither DCF nor HMP significantly correlated with the environmental parameters (Table S4). In addition, there was no significant correlation between DCF and HMP ( $r = -0.069$ ,  $p = 0.79$ ) (Figure 7), and the simple linear regression showed that the HMP explained only 2 % ( $R^2 = 0.02$ ) of the DCF variation. For the sediments, there was only a significant correlation between DCF and TOC ( $r = 0.41$ ,  $p = 0.05$ ), HMP

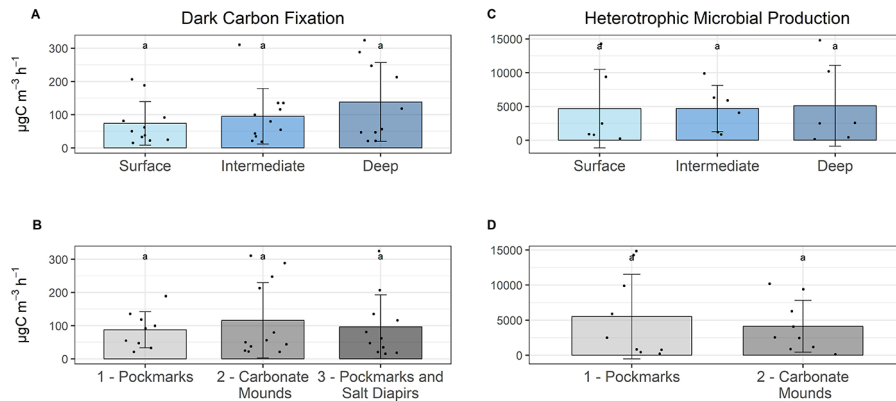


**Figure 3.** Average dark carbon fixation (DCF) ( $\mu\text{g C m}^{-3} \text{h}^{-1}$ ) of the water column per depths (A) and areas (B). Average heterotrophic microbial production (HMP) ( $\mu\text{g C m}^{-3} \text{h}^{-1}$ ) of the water column per depths (C) and areas (D). Points represent individual observations and the letters (a) indicate significant differences tested with ANOVA, same letters represent no significant difference ( $p > 0.05$ ). Data are expressed as mean  $\pm$  standard deviation.

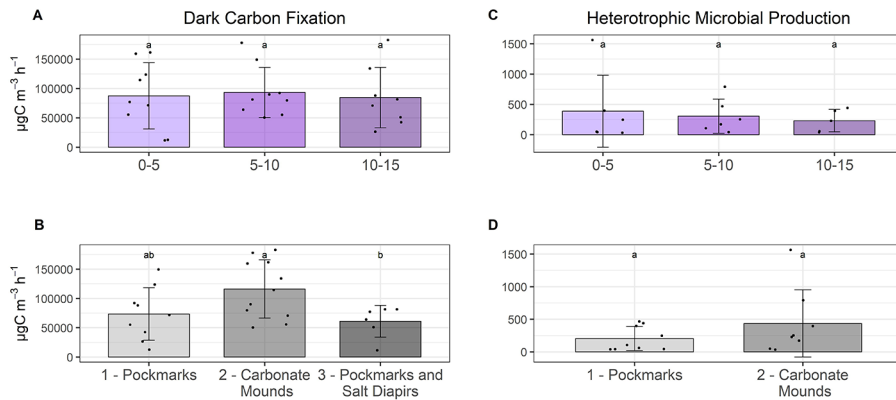


**Figure 4.** Average dark carbon fixation (DCF) ( $\mu\text{g C m}^{-3} \text{h}^{-1}$ ) of the sediment per layer (A) and areas (B). Average heterotrophic microbial production (HMP) ( $\mu\text{g C m}^{-3} \text{h}^{-1}$ ) of the sediment per layer (C) and areas (D). Points represent individual observations and the letters (a, b, ab) indicate significant differences tested with ANOVA, same letters represent no significant difference ( $p > 0.05$ ). Data are expressed as mean  $\pm$  standard deviation.

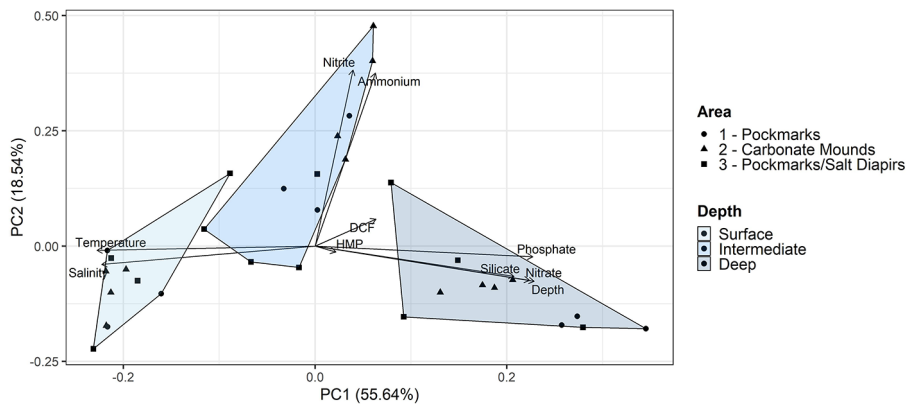


**Figure 5.** Principal component analysis (PCA) of the water samples on a factor plane and the vectors for dark carbon fixation (DCF), heterotrophic microbial production (HMP), depth, temperature, salinity, phosphate, silicate, nitrate, nitrite and ammonium.

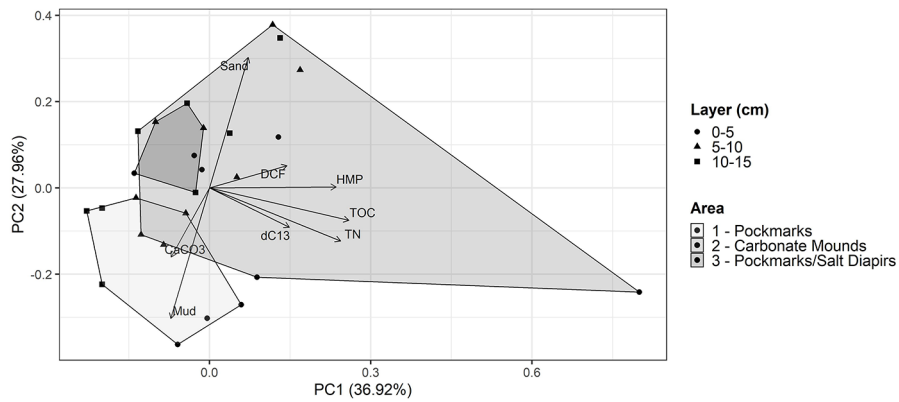


**Figure 6.** Principal component analysis (PCA) of the sediment samples on a factor plane and the vectors for dark carbon fixation (DCF), heterotrophic microbial production (HMP), sand, mud, calcium carbonate ( $CaCO_3$ ), total organic carbon (TOC),  $\delta^{13}C$ , total nitrogen (TN).

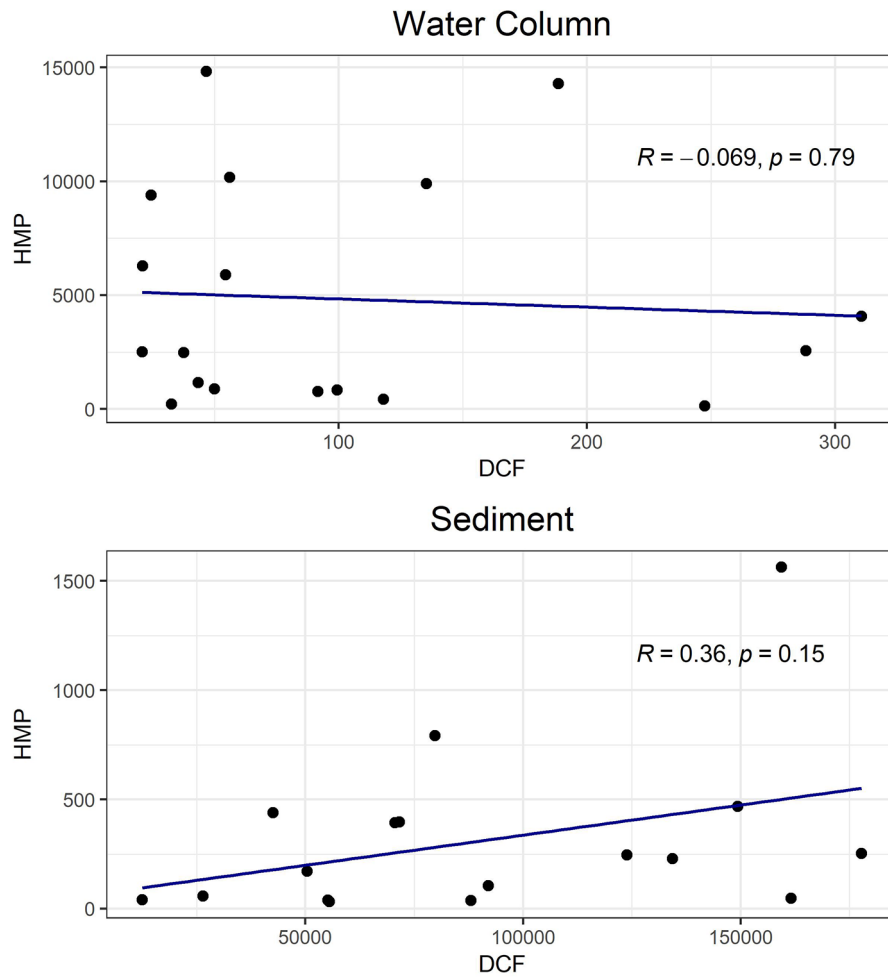


**Figure 7.** Scatter plot of the Pearson's correlation coefficient between the DCF and HMP ( $\mu g C m^{-3} h^{-1}$ ) for water column and sediment.

and TOC ( $r = 0.75$ ,  $p = 0.0007$ ) and TN ( $r = 0.71$ ,  $p = 0.0023$ ) (Figure 8, Table S5). In addition, the correlation between DCF and HMP rates was not significant ( $r = 0.36$ ,  $p = 0.15$ ) (Figure 7), with HMP explaining 18% ( $R^2 = 0.18$ ) of the DCF variation.

## DISCUSSION

### SPATIAL DISTRIBUTION PATTERNS OF ABIOTIC VARIABLES

Even though the PERMANOVA did not confirm the ordination between water depths observed in the PCA, the overall variation of the samples in the water column, including both the measured rates and environmental parameters, was based

on the latter, mostly the variables associated with the PC1. Vertical distribution of temperature and salinity matched with the typical T-S diagrams for the SW Atlantic Ocean (Cirano et al., 2006). The vertical distribution of phosphate, nitrate and silicate are explained by the high intake of nutrients by primary producers during photosynthesis in the photic layer (Suzuki et al., 2015; Bristow et al., 2017). Overall, the nutrient concentration was typical for the oligotrophic waters of the SW Atlantic Ocean, as those observed by Suzuki et al. (2015). The author reported phosphate, nitrate and silicate concentrations varying from undetected values to  $1.9 \mu\text{mol L}^{-1}$ ,  $5$  to  $27 \mu\text{mol L}^{-1}$  and  $1.3$  to  $22 \mu\text{mol L}^{-1}$ , respectively; there were no disclosed values

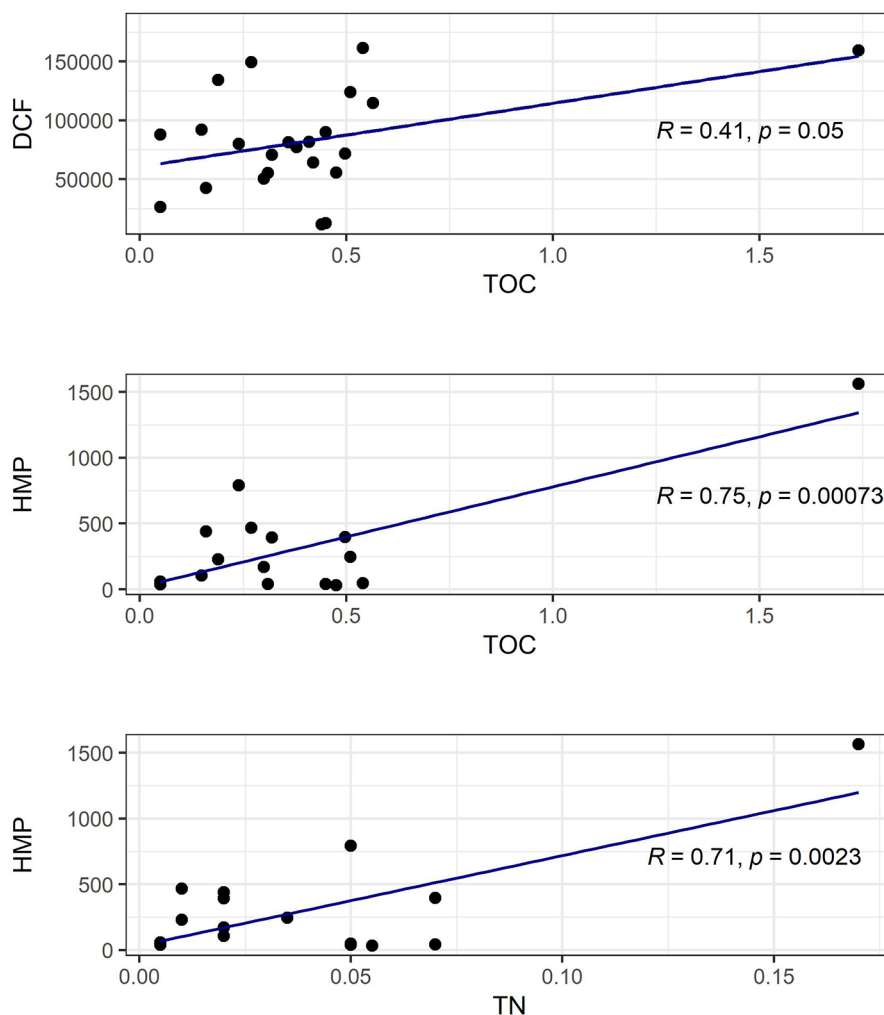


**Figure 8.** Scatter plot of the Pearson's correlation coefficient between the DCF ( $\mu\text{g C m}^{-3} \text{h}^{-1}$ ) and TOC (%); HMP ( $\mu\text{g C m}^{-3} \text{h}^{-1}$ ) and TOC and TN (%).

for nitrite, but the ammonium concentration was mostly undetected.

Although the use of the PCA was useful in reducing the dimension of our dataset, it was not enough to explain the variation of the DCF and HMP, as expected, since the environmental parameters did not influence the measured rates. Even though, in the water column, the chemoautotrophy relies on nitrogen compounds (Middelburg, 2011; Pachiadaki et al., 2017), this lack of correlation was also observed by Reinthaler et al. (2010) and Zhou et al. (2017). In the oxygenated dark ocean, there are other possible energy sources for the chemosynthesis, such as molecular hydrogen, nitrous oxide (Reinthaler et al., 2010), reduced sulfur compounds and methane (Swan et al., 2011), but these were not measured in this study. Additionally, it would have been relevant to measure the photosynthetic production or TOC in the water column, as they are most likely to affect the HMP (Azam et al., 1983).

In the SW Atlantic Ocean, the overall variation of sediment samples between areas was mostly dictated by variables associated with the PC2, including a separation of area A1 from the others due to a distinct sand and mud content. As expected, the areas comprising pockmarks and the carbonate mounds (Maly et al., 2019) revealed a higher carbonate content. Furthermore, the variation of the samples was also influenced by the organic matter in the sediments. The heterotrophic microorganisms are known to use organic matter as an energy source (Azam et al., 1983; Fukami et al., 1983), thus the observed effect of the TOC and TN in the HMP. Additionally, the TOC concentrations were low when compared with Santos et al. (2020); who obtained mean values of  $1.02 \pm 0.49$  %, while we had means of  $0.4 \pm 0.33$  %. The authors studied the continental margin of the SW Atlantic, with depths ranging from 10 to 300 m, which are shallower regions than ours. The distribution of TOC in deep sediments is usually attributed to photosynthetic production (Seiter et al., 2004), thus the lower TOC in deeper regions could be explained by the remineralization of the organic carbon in the water column (Middelburg, 1989; Wakeham et al., 1997; Del Giorgio and Duarte, 2002). Further, the  $\delta^{13}\text{C}$  value is also related with

the organic matter, as it provides an insight into its origin, since different sources of carbon have contrasting values of  $^{13}\text{C}$  (Meyers, 1994). Values of  $-22$  and  $-20$ ‰, such as those of this study, are related to marine organic matter, thus indicating that the organic matter that reaches the sediments could have its origin in the phytoplankton (Meyers, 1994).

One sampling location stood out from the others, the ST 685 (area A2), which can be considered an outlier, however, we have chosen to keep it in our data. This station presented higher values of TOC, TN and HMP, representing an influential outlier for the correlations mentioned above (Figure 8). We argue that this is a naturally occurring variation because the ST 685 is located on the eastern section of the Alpha Crucis Carbonate Ridge (ACCR) near the Besnard Mound, which is the highest peak of the ridge system (340 m above the seafloor) (Maly et al. 2019, Bendia et al., 2021). The ACCR is heavily influenced by the strong flow of the IWBC, which, combined with the BC, is the dominant mechanism of sediment transportation along the ocean floor off SE Brazil (Maly et al., 2019). Besides sediment, the ocean currents are capable of transporting nutrients and dissolved organic matter (Moriarty et al., 1995; Hansell et al., 2002; Schattner et al., 2020), which are closely related with TOC and TN, and consequently HMP.

A correlation between DCF and HMP could allude to the utilization of the labile organic matter from the DCF by the HMP or could also represent the fixation of inorganic carbon by heterotrophs. There are some uncertainties in the relevance of the DCF by heterotrophs to the carbon cycle due to methodological limitations in its measurement (Braun et al., 2021). Despite that, some studies associate this heterotrophic carbon fixation with anaplerotic reactions in the oligotrophic water column (González et al., 2008; Alonso-Sáez et al., 2010) and deep sea sediments (Braun et al., 2021), but this metabolism is linked with episodic events of increased input of organic matter (Baltar et al., 2016). The lack of a significant relationship between DCF and HMP may suggest that DCF by heterotrophs was not occurring at the time of sampling. However, remains unclear whether anaplerotic reactions were taking place, because

our data is not sufficient to make affirmations in this regard, as TOC in the water column was not measured and the method utilized in this study measures the total dark carbon fixation, without differentiating the pathways used.

### SPATIAL DISTRIBUTION OF MICROBIAL PROCESS IN THE PELAGIC AND BENTHIC SYSTEMS

There is a wide variation in the rates of microbial processes across the ocean; Middelburg (2011) stipulates that the chemoautotrophy in the water column occur mainly in the open ocean. However, in our study, the DCF rates found in the water column of the continental slope showed to be similar to those found in the Northwest Pacific Ocean (Zhou et al., 2017) and two to five orders of magnitude higher than the open ocean of the Tropical and North Atlantic (Reinthal et al., 2010; Berguauer et al. 2013; Baltar et al., 2016; La Cono et al., 2018) (Table 3). Clark et al. (2008) measured nitrite and ammonium concentration of the euphotic zone of the central North Atlantic and Tropical Atlantic. The author observed concentrations of nitrite to be fairly constant and less than  $0.005 \mu\text{mol L}^{-1}$  for both areas; and concentrations of ammonium were  $\sim 0.02$  and  $\sim 0.08 \mu\text{mol L}^{-1}$ ,

respectively. We observed higher concentrations in our study, particularly for nitrite, and considering that, in the ocean, nitrite-oxidizing bacteria has a great impact in the chemosynthesis (Pachiadaki et al., 2017), these differences seen above could be in reference to the concentrations of nutrients.

To compare chemosynthesis in sediments with other studies, we integrated DCF rates for the entire sediment layer (0 - 15 cm), resulting in values of 5510.69 to 19366.25  $\mu\text{g C m}^{-2} \text{h}^{-1}$ . When compared with deep sea sediments of the Northeast Atlantic Ocean (Pimenov et al., 2000), our rates were three to four orders of magnitude higher (Table 3). Chemoautotrophy in sediments relies mainly on the oxidation of reduced metabolites produced during anaerobic degradation of organic matter (Jørgensen, 1982; Middelburg, 2011), which could be the reason for the significant correlation between DCF and TOC. Coastal and slope sediments have already shown to have a higher organic carbon input (Deininger and Frigstad, 2019), for this reason they are the principal location of chemoautotrophy in ocean sediments (Middelburg, 2011). Another factor to be considered is the difference of temperature, as it affects the rate of metabolic processes in the ocean (Brown et al., 2004). However, there are

**Table 3.** Comparison of dark carbon fixation (DCF) and heterotrophic microbial production (HMP) rates of SW Atlantic Ocean from the present work and other studies.

Location	Type	DCF <sup>1</sup>	HMP <sup>1</sup>	Reference
Southwest Atlantic	Water	$4.2 \times 10^{-4}$	$4.8 \times 10^{-3}$	Present study
Southwest Atlantic	Sediment	$4.7 \times 10^2$	$3.9 \times 10^{-4}$	Present study
Mediterranean Sea	Water	9.3		La Cono et al., 2018
NW Mediterranean Sea	Water		$8.7 \times 10^{-5}$	Lemée et al., 2002
South China Sea	Water	$1.4 \times 10^{-4}$	$3.0 \times 10^{-5}$	Zhou et al., 2017
North-east Atlantic	Water	15		La Cono et al., 2018
Tropical Atlantic	Water	3		Bergauer et al. 2013
North Sea	Sediment		$3.4 \times 10^3$	Van Duyl et al., 1993
Coral and Solomon Sea	Sediment		72	Alongi et al., 1990
North Atlantic	Water	1.3		Reinthal et al., 2010
North Atlantic Mesopelagic	Water		$2.4 \times 10^{-1}$	Baltar et al., 2016
Island of Sylt (Germany)	Sediment	24		Evrard et al., 2008
Norwegian Sea	Sediment	$2.0 \times 10^6$		Pimenov et al., 2000
Southern Pacific Ocean	Water		$3.9 \times 10^{-7}$	Van Wambeke et al., 2008

<sup>1</sup>DCF and HMP unit rates are  $\mu\text{g C m}^{-3} \text{h}^{-1}$  for water samples and  $\mu\text{g C m}^{-2} \text{h}^{-1}$  for sediment samples.

still few studies on microbial processes in marine sediments in order to make a broader comparison between DCF rates in the SW Atlantic Ocean and other ocean regions.

The A2, where we observed relative higher rates of DCF in the sediments, include the Alpha Crucis Carbonate Ridge (ACCR) described by Maly et al. (2019). Although no active cold seep has been found in the Santos Basin, their study suggests that the ACCR is a unique feature likely influenced by the occurrence of recent to sub-recent active seepage, which can create an environment rich in methane and reduced sulfur compounds, potentially leading to higher DCF (Levin et al., 2016). Even in non-seep areas, such as the usual benthic environment the chemosynthetic processes are intensified due to the naturally occurring reduced compounds in marine sediments (Whiticar, 1990; Orcutt et al., 2011), which may explain the higher overall DCF rates when compared to the water column. This pattern is corroborated by the global estimates made by Middelburg (2011), where DCF rates in the continental slope sediments are higher than those of the water column above.

Heterotrophic production in the water column found in this study were one to two orders of magnitude higher than in the the Northwest Pacific Ocean (Zhou et al., 2017) and one to six orders higher than the Subtropical and North Atlantic (Aristegui et al., 2005; Reinthaler et al., 2010; Baltar et al., 2016; La Cono et al., 2018) (Table 3). To compare the HMP rates in sediments globally, we integrated HMP rates for all sediment layers (0 - 15 cm), resulting in values of 22.31 to 90.82  $\mu\text{g C m}^{-2} \text{h}^{-1}$ . This rate was similar to those of the deep sea in the Southwest Pacific Ocean (Alongi et al., 1990), but two orders of magnitude lower than coastal sediments of the Northeast Atlantic Ocean (Van Duyl and Kop, 1994) (Table 3). This pattern is probably because HMP is highly associated with organic matter, and coastal sediments have much greater input due to its proximity to the continent, which is a major source of the organic matter (Suzuki et al., 2015; Deininger and Frigstad, 2019).

The distribution of HMP exhibited an opposite trend to the DCF, with higher rates in the water

column than in the sediments, probably because the heterotrophic processes are mainly driven by the organic matter input (Azam et al., 1983; Fukami et al., 1983). Since the continental input of organic matter is rather low in the Santos Basin (de Mahiques et al., 2004), the HMP would be strongly affected by the local photosynthetic production. This is reflected by a higher HMP in the surface and lower in the sediment, as only a limited amount of organic matter reaches the seafloor due to its remineralization in the mesopelagic zone (Del Giorgio and Duarte, 2002). Hence the lower TOC found in the sediment and consequently the lower HMP rates. In addition, the  $\delta^{13}\text{C}$  values of the sediments support phytoplankton production as the main source of organic matter.

## RELATIVE IMPORTANCE OF CHEMOSYNTHESIS IN THE DEEP SEA

Kutner et al. (2023) estimated the primary production for three areas of the Santos Basin: shelf, transition zone and open ocean; in which, the last two cover our study area. The production in the transition zone and open ocean were 1260 and 1020  $\mu\text{g C m}^{-3} \text{h}^{-1}$ , respectively, and they observed that the DCF represented, on average, 10.2 % of the total primary production. In our study, we estimated that the average DCF in the epipelagic was  $73.76 \pm 65.89 \mu\text{g C m}^{-3} \text{h}^{-1}$ , which represents 2.9 to 3.2 % of the primary production reported by (Kutner et al., 2023). Although our study did not measure photosynthetic rates and this comparison is somewhat speculative, these values are amongst the estimates of 2.5 to 22 % for the global epipelagic ocean (Baltar and Herndl, 2019). Thus, not only the DCF can be relevant to the epipelagic primary production, but also for meso- and bathypelagic zones, since the DCF can represents about 15 to 53 % of the carbon derived from phytoplankton production exported to the seafloor (Reinthaler et al., 2010).

## CONCLUSION

To our knowledge, it is the first study to investigate the spatial distribution of DCF and HMP both in pelagic and benthic microbial communities of an oligotrophic marine system. In this study, though it is not clear which metabolic pathway is

predominantly used in the fixation of dark carbon, the DCF can represent a significant percentage of the total primary production in the euphotic water column. The DCF rates are relatively high in the Santos Basin, with patterns of higher rates in the sediments than in the water column above, which are aligned with higher amounts of reduced compounds in the sediment; the HMP had an opposite pattern, likely due to the decrease of available organic matter with depth. What drives the chemosynthesis in the ocean remains to be investigated; in further studies, it would be important to investigate the influence of different parameters related with DCF, such as the concentration of other reduced compounds associated with this metabolism. The oligotrophic South Atlantic Ocean is amongst the least known ocean basins, and, although a geographically broader set of measurements is required to refine the estimates in the region, this study provides important new data regarding the microbial processes herein studied. Finally, we reinforce the need for DCF rates to be included in ecological studies that assess the carbon balance in the SW Atlantic Ocean, as it represents an important aspect of primary production in both the water column and sediments.

## ACKNOWLEDGMENTS

This research was carried out in association with the ongoing R&D project registered as ANP 21012-0, “MARINE LIFE - BMC - OIL AND GAS SEEPS (BIOIL)” (Universidade de São Paulo / Shell Brasil / ANP) – Avaliação da Biologia e Geoquímica de Exsudações de Óleo e Gás na Costa Sudeste do Brasil, sponsored by Shell Brasil under the ANP R&D levy à “Compromisso de Investimentos com Pesquisa e Desenvolvimento”. We would like to thank Dr. Flávia Saldanha-Corrêa, MSc. Mayza Pompeu and MSc. Raissa B. Ramos for their scientific support and we also thank Captain Rezende and R/V Alpha Crucis crew. J.G.P. was supported by Master’s fellowships from the Federal Agency for the Support and Evaluation of Graduate Education - CAPES. L.S.F.’s Scientific Initiation fellowship was supported by BIOIL Project (Shell Brasil) through Fundação de Apoio a Universidade de São Paulo (FUSP).

## AUTHOR CONTRIBUTIONS

J.G.P., L.F.S.: Conceptualization; Methodology; Formal Analysis; Writing – original draft; Writing – review & editing.  
 P.Y.G.S.: Project Administration; Funding Acquisition; Resources; Writing – review & editing.  
 A.G.B., F.M.N.: Writing – review & editing.  
 V.H.P.: Conceptualization; Writing – review & editing.  
 C.N.S.: Conceptualization; Methodology; Resources; Supervision; Writing – review & editing.

## REFERENCES

- ALONGI, D. M. 1990. Bacterial growth rates, production and estimates of detrital carbon utilization in deep-sea sediments of the Solomon and Coral Seas. *Deep Sea Research Part A. Oceanographic Research Papers*, 37(5), 731-746.
- ALONSO-SÁEZ, L., GALAND, P. E., CASAMAYOR, E. O., PEDROS-ALIO, C. & BERTILSSON, S. 2010. High bicarbonate assimilation in the dark by Arctic bacteria. *The ISME Journal*, 4(12), 1581-1590.
- ARÍSTEGUI, J., DUARTE, C. M., GASOL, J. M. & ALONSO-SÁEZ, L. 2005. Active mesopelagic prokaryotes support high respiration in the subtropical northeast Atlantic Ocean. *Geophysical Research Letters*, 32(3), L03608.
- AZAM, F., FENCHEL, T., FIELD, J. G., GRAY, J. S., MEYER-REIL, L. A. & THINGSTAD, F. 1983. The ecological role of water-column microbes in the sea. *Marine Ecology Progress Series*, 10, 257-263.
- BALTAR, F. & HERNDL, G. J. 2019. Ideas and perspectives: is dark carbon fixation relevant for oceanic primary production estimates? *Biogeosciences*, 16(19), 3793-3799.
- BALTAR, F., LUNDIN, D., PALOVAARA, J., LEKUNBERRI, I., REINTHALER, T., HERNDL, G. J. & PINHASSI, J. 2016. Prokaryotic responses to ammonium and organic carbon reveal alternative CO<sub>2</sub> fixation pathways and importance of alkaline phosphatase in the mesopelagic North Atlantic. *Frontiers in Microbiology*, 7, 1670.
- BENDIA, A. G., NAKAMURA, F. M., BUTARELLI, A. C. D. A., KMIT, M. C. P., RAMOS, R. B., SIGNORI, C. N., LOURENÇO, R. A., DE MAHIQUES, M. M., SUMIDA, P. Y. G. & PELLIZARI, V. H. 2022. First description of archaeal communities in carbonate-rich seafloor and subseafloor sediments from the Southwestern Atlantic slope. *Ocean and Coast Research*, 70(Suppl 2), e22047.
- BENDIA, A. G., SIGNORI, C. N., NAKAMURA, F. M., BUTARELLI, A. C. D. A., PASSOS, J. G., RAMOS, R. B., SOARES, L. F., DE MAHIQUES, M. M., SUMIDA, P. Y. G. & PELLIZARI, V. H. 2021. Microbial perspective on the giant carbonate ridge Alpha Crucis (Southwestern Atlantic upper slope). *FEMS Microbiology Ecology*, 97(8), p.fiab110.
- BERG, C., LISTMANN, L., VANDIEKEN, V., VOGTS, A. & JURGENS, K. 2014. Chemoautotrophic growth of ammonia-oxidizing Thaumarchaeota enriched from a pelagic redox gradient in the Baltic Sea. *Frontiers in Microbiology*, 5, 786.

- BERGAUER, K., SINTES, E., VAN BLEIJSWIJK, J., WITTE, H. & HERNDL, G. J. 2013. Abundance and distribution of archaeal acetyl-CoA/propionyl-CoA carboxylase genes indicative for putatively chemoautotrophic Archaea in the tropical Atlantic's interior. *FEMS Microbiology Ecology*, 84(3), 461-473.
- BERTINI, L. & BRAGA, E. 2022. The contribution of nutrients and water properties to the carbonate system in three particular areas of the Tropical Atlantic (NE-BRAZIL). *Journal of Geoscience and Environment Protection*, 10(2), 135-161.
- BOEBEL, O., SCHMID, C. & ZENK, W. 1997. Flow and recirculation of Antarctic intermediate water across the Rio Grande rise. *Journal of Geophysical Research: Oceans*, 102(C9), 20967-20986.
- BRAUN, A., SPONA-FRIEDL, M., AVRAMOV, M., ELSNER, M., BALTAR, F., REINTHALER, T., HERNDL, G. J. & GRIEBLER, C. 2021. Reviews and syntheses: heterotrophic fixation of inorganic carbon—significant but invisible flux in environmental carbon cycling. *Biogeosciences*, 18(12), 3689-3700.
- BRISTOW, L. A., MOHR, W., AHMERKAMP, S. & KUYPERS, M. M. 2017. Nutrients that limit growth in the ocean. *Current Biology*, 27(11), R474-R478.
- BROWN, J. H., GILLOOLY, J. F. & ALLEN, A. P., SAVAGE V. M. & WEST, G. B. 2004. Toward a metabolic theory of ecology. *Ecology*, 85(7), 1771-1789.
- CIRANO, M., MATA, M. M., CAMPOS, E. J. & DEIRÓ, N. F. 2006. A circulação oceânica de larga-escala na região oeste do Atlântico Sul com base no modelo de circulação global OCCAM. *Revista Brasileira de Geofísica*, 24(2), 209-230.
- CLARK, D. R., REES, A. P. & JOINT, I. 2008. Ammonium regeneration and nitrification rates in the oligotrophic Atlantic Ocean: implications for new production estimates. *Limnology and Oceanography*, 53(1), 52-62.
- DAS, A., SUJITH, P. P., MOURYA, B. S., BICHE, S. U. & LOKABHARATHI, P. A. 2011. Chemosynthetic activity prevails in deep-sea sediments of the Central Indian Basin. *Extremophiles*, 15(2), 177-189.
- DE MAHIQUES, M. M., SCHATTNER, U., LAZAR, M., SUMIDA, P. Y. G. & SOUZA, L. A. P. 2017. An extensive pockmark field on the upper Atlantic margin of Southeast Brazil: spatial analysis and its relationship with salt diapirism. *Heliyon*, 3(2), e00257.
- DE MAHIQUES, M. M., TESSLER, M. G., CIOTTI, A. M., SILVEIRA, I. C. A., E SOUSA, S. H. D. M., FIGUEIRA, R. C. L., TASSINARI, C. C. G., FURTADO, V. V. & PASSOS, R. F. 2004. Hydrodynamically driven patterns of recent sedimentation in the shelf and upper slope off Southeast Brazil. *Continental Shelf Research*, 24(15), 1685-1697.
- DEININGER, A. & FRIGSTAD, H. 2019. Reevaluating the role of organic matter sources for coastal eutrophication, oligotrophication, and ecosystem health. *Frontiers in Marine Science*, 6, 210.
- DEL GIORGIO, P. A. & DUARTE, C. M. 2002. Respiration in the open ocean. *Nature*, 420(6914), 379-384.
- DYSKMA, S., BISCHOF, K., FUCHS, B. M., HOFFMANN, K., MEIER, D., MEYERDIERKS, A., PJEVAC, P., PROBANDT, D., RICHTER, M., STEPANAUSKAS, R. & MUßMANN, M. 2016. Ubiquitous Gammaproteobacteria dominate dark carbon fixation in coastal sediments. *The ISME Journal*, 10(8), 1939-1953.
- FOX, J. & WEISBERG, S. 2019. *An R companion to applied regression*. 3<sup>rd</sup> ed. Thousand Oaks: Sage.
- FRAZÃO, L. R., PENNINGCK, S. B., MICHELAZZO, L. S., MORENO, G., GUIMARÃES, C., LOPES, R. M. & SIGNORI, C. N. 2021. Microbial ecology of the South Atlantic Subtropical Gyre: a state-of-the-art review of an understudied ocean region. *Ocean and Coastal Research*, 69, e21027.
- FUKAMI, K., SIMIDU, U. & TAGA, N. 1983. Distribution of heterotrophic bacteria in relation to the concentration of particulate organic matter in seawater. *Canadian Journal of Microbiology*, 29(5), 570-575.
- GONZÁLEZ, J. M., FERNÁNDEZ-GÓMEZ, B., FERNÁNDEZ-GUERRA, A., GÓMEZ-CONSARNAU, L., SÁNCHEZ, O., COLL-LLADÓ, M., DEL CAMPO, J., ESCUDERO, L., RODRÍGUEZ-MARTÍNEZ, R., ALONSO-SÁEZ, L., LATASA, M., PAULSEN, I., NEDASHKOVSKAYA, O., LEKUNBERRI, I., PINHASSI, J. & PEDRÓS-ALIÓ, C. 2008. Genome analysis of the proteorhodopsin-containing marine bacterium *Polaribacter* sp. MED152 (Flavobacteria). *Proceedings of the National Academy of Sciences*, 105(25), 8724-8729.
- GRASSHOFF, K., KREMLING, K. & EHRHARDT, M. 2009. *Methods of seawater analysis*. London: John Wiley & Sons.
- HANSELL, D. A., CARLSON, C. A. & SUZUKI, Y. 2002. Dissolved organic carbon export with North Pacific Intermediate Water formation. *Global Biogeochemical Cycles*, 16(1), 7-1.
- HÜGLER, M. & SIEVERT, S. M. 2011. Beyond the Calvin cycle: autotrophic carbon fixation in the ocean. *Annual Review of Marine Science*, 3, 261-289.
- ISO (International Standardization Organization). 2009. *ISO13320:2009. Particle size analysis. Laser diffraction methods*. Publication 2009 October 01. Geneva: ISO, pp. 1-51. Available at: [http://www.iso.org/iso/catalogue\\_detail.htm?csnumber=44929](http://www.iso.org/iso/catalogue_detail.htm?csnumber=44929) [Accessed: 5 Jul 2021].
- JØRGENSEN, B. B. 1982. Mineralization of organic matter in the sea bed - the role of sulfate reduction. *Nature*, 296, 643-645.
- KIRCHMAN, D., K'NEES, E. & HODSON, R. 1985. Leucine incorporation and its potential as a measure of protein synthesis by bacteria in natural aquatic systems. *Applied and Environmental Microbiology*, 49(3), 599-607.
- KUTNER, D. S., BOWMAN, J. S., SALDANHA-CORRÊA, F. M. P., CHUQUI, M. G., TURA, P. M., MOREIRA, D. L., BRANDINI, F. P. & SIGNORI, C. N. 2023. Inorganic carbon assimilation by planktonic community in Santos Basin, Southwestern Atlantic Ocean. *Ocean and Coastal Research*, 71(Suppl 3), e23006.

- LA CONO, V., RUGGERI, G., AZZARO, M., CRISAFI, F., DECEMBRINI, F., DENARO, R., LA SPADA, G., MAIMONE, G., MONTICELLI, L. S., SMEDILE, F., GIULIANO, L. & YAKIMOV, M. M. 2018. Contribution of bicarbonate assimilation to carbon pool dynamics in the deep Mediterranean Sea and cultivation of actively nitrifying and CO<sub>2</sub>-fixing bathypelagic prokaryotic consortia. *Frontiers in Microbiology*, 9, 3.
- LEVIN, L. A., BACO, A. R., BOWDEN, D. A., COLACO, A., CORDES, E. E., CUNHA, M. R., DEMOPOULOS, A. W., GOBIN, J., GRUPE, B. M., LE, J., METAXAS, A., NETBURN, A. N., ROUSE, G. W., THURBER, A. R., TUNNICLIFFE, V., VAN DOVER, C. L., VANREUSEL, A. & WATLING, L. 2016. Hydrothermal vents and methane seeps: rethinking the sphere of influence. *Frontiers in Marine Science*, 3, 72.
- LEVIN, L. A., BETT, B. J., GATES, A. R., HEIMBACH, P., HOWE, B. M., JANSSEN, F., MCCURDY, A., RUHL, H. A., SNELGROVE, P., STOCKS, K. I., BAILEY, D., BAUMANN-PICKERING, S., BEAVERSON, C., BENFIELD, M. C., BOOTH, D. J., CARREIRO-SILVA, M., COLAÇO, A., EBLÉ, M. C., FOWLER, A. M., GJERDE, K. M., JONES, D. O. B., KATSUMATA, K., KELLEY, D., LE BRIS, N., LEONARDI, A. P., LEJZEROWICZ, F., MACREADIE, P. I., MCLEAN, D., MEITZ, F., MORATO, T., NETBURN, A., PAWLOWSKI, J., SMITH, C. R., SUN, S., UCHIDA, H., VARDARO, M. F., VENKATESAN, R. & WELLER, R. A. 2019. Global observing needs in the deep ocean. *Frontiers in Marine Science*, 6, 241.
- MALY, M., SCHATTNER, U., LOBO, F. J., DIAS, R. J. S., RAMOS, R. B., COUTO, D. M., SUMIDA, P. Y. G. & DE MAHIQUES, M. M. 2019. The Alpha Crucis Carbonate Ridge (ACCR): discovery of a giant ring-shaped carbonate complex on the SW Atlantic margin. *Scientific Reports*, 9(1), 1-11.
- MCNICHOL, J., STRYHANYUK, H., SYLVA, S. P., THOMAS, F., MUSAT, N., SEEWALD, J. S. & SIEVERT, S. M., 2018. Primary productivity below the seafloor at deep-sea hot springs. *Proceedings of the National Academy of Sciences*, 115(26), 6756-6761.
- MEYERS, P. A. 1994. Preservation of elemental and isotopic source identification of sedimentary organic matter. *Chemical Geology*, 114(3-4), 289-302.
- MIDDELBURG, J. J. 1989. A simple rate model for organic matter decomposition in marine sediments. *Geochimica et Cosmochimica Acta*, 53(7), 1577-1581.
- MIDDELBURG, J. J. 2011. Chemoautotrophy in the ocean. *Geophysical Research Letters*, 38(24), L24604.
- MOLARI, M., MANINI, E. & DELL'ANNO, A. 2013. Dark inorganic carbon fixation sustains the functioning of benthic deep-sea ecosystems. *Global Biogeochemical Cycles*, 27(1), 212-221.
- MORIARTY, D. J. W. & O'DONOHUE, M. J. 1995. Organic carbon transport from the Southern Ocean and bacterial growth in the Antarctic Intermediate Water masses of the Tasman Sea. *Marine Ecology Progress Series*, 119(1-3), 291-297.
- OKSANEN, J., BLANCHET, F. G., FRIENDLY, M., KINDT, R., LEGENDRE, P., MCGLINN, D., MINCHIN, P. R., O'HARA, R. B., SIMPSON, G. L., SOLYMOS, P., HENRY, M., STEVENS, H., SZOECES, E. & WAGNER, H. 2020. *Vegan: Community Ecology Package. R package version 2.5-7*. Vienna: R Foundation for Statistical Computing. Available at: <https://CRAN.R-project.org/package=vegan> [Accessed: 25 Nov 2020].
- ORCUTT, B. N., SYLVAN, J. B., KNAB, N. J. & EDWARDS, K. J. 2011. Microbial ecology of the dark ocean above, at, and below the seafloor. *Microbiology and Molecular Biology Reviews*, 75(2), 361-422.
- PACHIADAKI, M. G., SINTES, E., BERGAUER, K., BROWN, J. M., RECORD, N. R., SWAN, B. K., MATHYER, M. E., HALLAM, S. J., LOPEZ-GARCIA, P., TAKAKI, Y. & NUNOURA, T. 2017. Major role of nitrite-oxidizing bacteria in dark ocean carbon fixation. *Science*, 358(6366), 1046-1051.
- PIMENOV, N. V., SAVVICHEV, A. S., RUSANOV, I. I., LEIN, A. Y. & IVANOV, M. V. 2000. Microbiological processes of the carbon and sulfur cycles at cold methane seeps of the North Atlantic. *Microbiology*, 69(6), 831-843.
- R CORE TEAM. 2020. *R: A language and environment for statistical computing*. Vienna: R Foundation for Statistical Computing. Available at: <https://www.R-project.org/> [Accessed: 10 Out 2020].
- RAMOS, R. B., SANTOS, R. F., SCHATTNER, U., FIGUEIRA, R. C. L., BÍCEGO, M. C., LOBO, F. J. & DE MAHIQUES, M. M. 2019. Deep pockmarks as natural sediment traps: a case study from southern Santos Basin (SW Atlantic upper slope). *Geo-Marine Letters*, 40, 989-999.
- REINTHALER, T., VAN AKEN, H. M. & HERNDL, G. J. 2010. Major contribution of autotrophy to microbial carbon cycling in the deep North Atlantic's interior. *Deep Sea Research Part II: Topical Studies in Oceanography*, 57(16), 1572-1580.
- ROMANENKO, V. I. 1964. Heterotrophic assimilation of CO<sub>2</sub> by bacterial flora of water. *Mikrobiologiya*, 33, 610-613.
- SANTORO, A. L., BASTVIKEN, D., GUDASZ, C., TRANVIK, L. & ENRICH-PRAST, A. 2013. Dark carbon fixation: an important process in lake sediments. *PLoS One*, 8(6), e65813.
- SANTOS, F. R., NEVES, P. A., KIM, B. S., TANIGUCHI, S., LOURENÇO, R. A., TIMOSZCZUK, C. T., SOTÃO, B. M., MONTONE, R. C., FIGUEIRA, R. C., MAHIQUES, M. M. & BÍCEGO, M. C. 2020. Organic contaminants and trace metals in the western South Atlantic upper continental margin: anthropogenic influence on mud depocenters. *Marine Pollution Bulletin*, 154, 111087.
- SAVICHEV, A. S., KADNIKOV, V. V., KRAVCHISHINA, M. D., GALKIN, S. V., NOVIGATSKII, A. N., SIGALEVICH, P. A., MERKEL, A. Y., RAVIN, N. V., PIMENOV, N. V. & FLINT, M. V. 2018. Methane as an organic matter source and the trophic basis of a Laptev sea cold seep microbial community. *Geomicrobiology Journal*, 35(5), 411-423.

- SCHATTNER, U., LAZAR, M., SOUZA, L. A. P., TEN BRINK, U. & DE MAHIQUES, M. M. 2016. Pockmark asymmetry and seafloor currents in the Santos Basin offshore Brazil. *Geo-Marine Letters*, 36, 457-464.
- SCHATTNER, U., LOBO, F. J., GARCÍA, M., KANARI, M., RAMOS, R. B. & DE MAHIQUES, M. M. 2018. A detailed look at diapir piercement onto the ocean floor: new evidence from Santos Basin, offshore Brazil. *Marine Geology*, 406, 98-108.
- SCHATTNER, U., LOBO, F. J., LÓPEZ-QUIRÓS, A., NASCIMENTO, J. L. P. & DE MAHIQUES, M. M. 2020. What feeds shelf-edge clinoforms over margins deprived of adjacent land sources? An example from southeastern Brazil. *Basin Research*, 32(2), 293-301.
- SEITER, K., HENSEN, C., SCHRÖTER, J. & ZABEL, M. 2004. Organic carbon content in surface sediments—defining regional provinces. *Deep Sea Research Part I: Oceanographic Research Papers*, 51(12), 2001-2026.
- SIGNORI, C. N., FELIZARDO, J. P. S. & ENRICH-PRAST, A. 2020. Bacterial production prevails over photo-and chemosynthesis in a eutrophic tropical lagoon. *Estuarine, Coastal and Shelf Science*, 243, 106889.
- SIGNORI, C. N., VALENTIN, J. L., POLLERY, R. C. & ENRICH-PRAST, A. 2018. Temporal variability of dark carbon fixation and bacterial production and their relation with environmental factors in a tropical estuarine system. *Estuaries and Coasts*, 41(4), 1089-1101.
- SILVEIRA, I. C. A. D., SCHMIDT, A. C. K., CAMPOS, E. J. D., GODOI, S. S. D. & IKEDA, Y. 2000. A corrente do Brasil ao largo da costa leste brasileira. *Revista Brasileira de Oceanografia*, 48(2), 171-183.
- SIMON, M. & AZAM, F. 1989. Protein content and protein synthesis rates of planktonic marine bacteria. *Marine Ecology Progress Series*, 51, 201-213.
- SMITH, D. C. & AZAM, F. 1992. A simple, economical method for measuring bacterial protein synthesis rates in seawater using <sup>3</sup>H-leucine. *Marine Microbial Food Webs*, 6(2), 107-114.
- SOROKIN, D. Y. 1993. Influence of thiosulfate on activity of carbon dioxide assimilation by marine heterotrophic thiosulfate-oxidizing bacteria. *Microbiology*, 62 (5), 488-493.
- STEEMANN-NIELSEN, E. 1952. The use of radio-active carbon (C14) for measuring organic production in the sea. *ICES Journal of Marine Science*, 18(2), 117-140.
- SUMIDA, P. Y. G., PELLIZARI, V. H., LOURENÇO, R. A., SIGNORI, C. A., BENDIA, A. G., CARRETTE, O., NAKAMURA, F. M., RAMOS, R. B., BERGAMO, B., SOUZA, B. H. M., BUTARELLI, A. C. A., PASSOS, J. G., DIAS, R. J., MALY, M., BANHA, T. N. S., GUTH, A. Z., SOARES, L. F., PERUGINO, P. D. N., SANTOS, F. R., SANTANA, F. R. & DE MAHIQUES, M. M. 2022. Seep hunting in the Santos Basin, Southwest Atlantic: sampling strategy and employed methods of the multidisciplinary cruise BIOIL 1. *Ocean and Coastal Research*, 70(Suppl 2), e22031.
- SUZUKI, M. S., REZENDE, C. E., PARANHOS, R. & FALCÃO, A.P. 2015. Spatial distribution (vertical and horizontal) and partitioning of dissolved and particulate nutrients (C, N and P) in the Campos Basin, Southern Brazil. *Estuarine, Coastal and Shelf Science*, 166(Pt A), 4-12.
- SVENSSON, J. M., ENRICH-PRAST, A. & LEONARDSON, L. 2001. Nitrification and denitrification in a eutrophic lake sediment bioturbated by oligochaetes. *Aquatic Microbial Ecology*, 23(2), 177-186.
- SWAN, B. K., MARTINEZ-GARCIA, M., PRESTON, C. M., SCZYRBA, A., WOYKE, T., LAMY, D., REINTHALER, T., POULTON, N. J., MASLAND, E. D. P., GOMEZ, M. L. & SIERACKI, M.E. 2011. Potential for chemolithoautotrophy among ubiquitous bacteria lineages in the dark ocean. *Science*, 333(6047), 1296-1300.
- TEIXEIRA, C. 1973. Introdução aos métodos para medir a produção primária do fitoplâncton marinho. *Boletim do Instituto Oceanográfico*, 22, 59-92.
- VAN DUYL, F. C. & KOP, A. J. 1994. Bacterial production in North Sea sediments: clues to seasonal and spatial variations. *Marine Biology*, 120(2), 323-337.
- WAKEHAM, S. G., LEE, C., HEDGES, J. I., HERNES, P. J. & PETERSON, M. J. 1997. Molecular indicators of diagenetic status in marine organic matter. *Geochimica et Cosmochimica Acta*, 61(24), 5363-5369.
- WETZEL, R. G. & LIKENS, G. E. 1991. Limnological analyses. 2<sup>nd</sup> edn. New York, *Springer Science & Business Media*.
- ZHOU, W., LIAO, J., GUO, Y., YUAN, X., HUANG, H., YUAN, T. & LIU, S. 2017. High dark carbon fixation in the tropical South China Sea. *Continental Shelf Research*, 146, 82-88.